Temperature dependence of the vortex remanent state in high-T_c superconductors

Rongchao Ma, K. H. Chow, and J. Jung*
Department of Physics, University of Alberta, Edmonton, Alberta, Canada T6G 2G7

D. Prabhakaran
Clarendon Laboratory, Department of Physics, Oxford University, Parks Road, Oxford OX1 3PU, United Kingdom

H. Tadatomo, T. Masui, and S. Tajima
Department of Physics, Osaka University, Osaka 560-0043, Japan

(Received 1 October 2010; revised manuscript received 21 March 2011; published 20 June 2011)

Temperature and magnetic field dependence of the vortex penetration into a superconductor and the resulting trapped vortex field (the vortex remanent state) were investigated for $Bi_2Sr_2CaCu_2O_{8+x}$ (BSCCO) and $YBa_2Cu_3O_{6+x}$ (YBCO) single crystals and BSCCO thin films. The experiments revealed changes in the pinning regime (the magnitude and magnetic relaxation) of the trapped vortex field with an increasing temperature. The trapped vortex field, obtained by applying a constant magnetic field, exhibits a maximum at a certain temperature, that separates the partial vortex penetration regime at low temperatures from the complete vortex penetration state at higher temperatures. The corresponding vortex remanent states in these two regimes are characterized by two distinctly different relaxations, the logarithmic and the nonlogarithmic ones at temperatures below and above the maximum, respectively, for both BSCCO and YBCO. At temperatures close to T_c surface/geometric barrier affect the relaxation rates.

DOI: 10.1103/PhysRevB.83.212504 PACS number(s): 74.25.Op, 74.25.Uv, 74.25.Wx

According to the Bean's model,[1] when an external magnetic field is applied to a superconductor, the internal magnetic field is not uniform and its local value depends on the position inside a superconductor.[2] When the external magnetic field is removed, a nonuniform vortex field is trapped in a superconductor. Trapping of the internal field inside a superconductor can be realized by using the following procedure:[3] apply an external magnetic field, H_a, to a superconductor at different temperatures, which results in the penetration of vortices into the bulk of the superconductor. H_a is subsequently reduced to zero and the vortex lines are trapped inside the sample. At a fixed temperature, the trapped magnetic field increases with an increasing H_a and finally reaches a saturated (remanent) value.[4] The remanent value of the trapped internal field is proportional to the critical current.

However, applying the same constant H_a at different temperatures leads to a different situation. In this case, the magnitude of the trapped internal field is determined by the dependence of the penetration and pinning of the vortices on temperature. At low temperatures, the sample is partly penetrated by the field and the internal field is trapped at the sample's edges. It is expected that the trapped internal field increases with an increasing temperature and at a certain temperature, fully penetrates the sample, i.e., reaches a maximum value at the sample's center. The question is, however, what is the magnitude and the temperature dependence of this field at higher temperatures? Does it follow the temperature dependence of the remanent critical state where the current density acquires the critical value J_c, or does it have a different temperature dependence? What are the relaxation rates of this field at temperatures corresponding to the partial and complete vortex penetration states? Are they affected by the surface/geometrical barriers? What is their dependence on the superconducting material?

The properties of the trapped field and its response to pinning complement our understanding of the vortex remanent state in different high-T_c superconductors and are the subject of the present investigations. They allow one to visualize how the trapped vortex lattice and its pinning evolves with an increasing temperature and an external magnetic field, and what happens to it when the critical state is approached.

These studies have been performed on $YBa_2Cu_3O_{6+x}$ (YBCO) crystal and $Bi_2Sr_2CaCu_2O_{8+x}$ (BSCCO) crystals and films characterized by different vortex pinning potentials. High purity BSCCO crystals of $T_c \simeq 92$ K were grown in the crystal-growth division of the Clarendon Laboratory (Oxford University) using a crucible-free optical floating-zone technique. The crystals were shaped in the form of about 0.5-mm thick disks and rings of outer diameters of 1.5 mm. The disk/ring axes were parallel to the c-axis of the crystal. Pure detwinned YBCO single crystal with T_c of 93.5 K and the dimensions of 2 mm $\times$ 3 mm $\times$ 0.5 mm (with the c-axis perpendicular to the plate) was prepared at Osaka University. BSCCO c-axis-oriented thin films of $T_c \simeq 82$ K were grown on (100) MgO substrates using magnetron sputter deposition technique. These films were patterned in the form of disks of thickness 220 nm and a diameter of 10 mm.

The trapping of vortices is produced by applying an external magnetic field H_a (up to 1.5 kG, generated by a copper-wound solenoid) to the zero-field-cooled samples at temperatures below T_c in a direction parallel to the c-axis (perpendicular to the sample's plane), and subsequently reducing this field to zero after a time interval t^*. Changes in the resulting trapped vortex field were monitored as a function of temperature, applied magnetic field, and time, as discussed in more detail below.

Magnetic fields due to the distributions of vortices trapped by a superconducting sample are equivalent to the self-fields

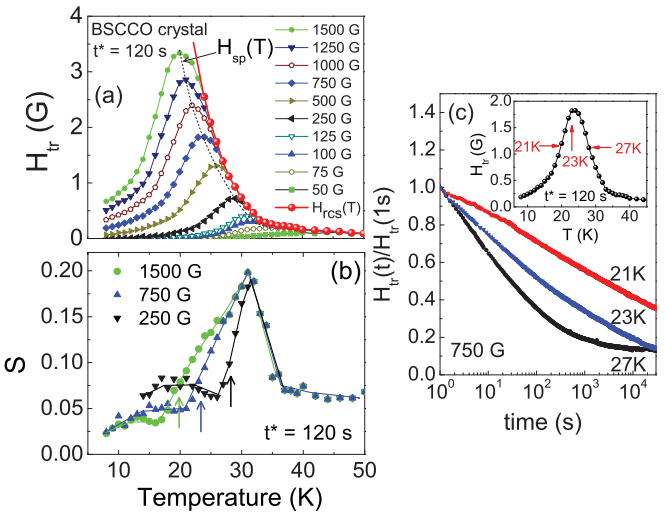

FIG. 1. (Color online) (a) Temperature dependence of the field trapped at the center of the BSCCO single crystal by applying different constant magnetic fields between 50 and 1500 G during a time interval t^* of 120 s. $H_{rcs}(T)$ represents the "remanent critical state" line. $H_{sp}(T)$ line joins the maxima of the trapped field. (b) Temperature dependence of the logarithmic decay rates $S = d(\ln H_{tr})/d(\ln t)$ of the trapped field calculated for a short initial time intervals up to 10–20 s. The arrows indicate temperatures at which the maxima in the trapped field occur. (c) Dependence of the field trapped in the BSCCO crystal on time measured at different temperatures around the maximum of the trapped field.

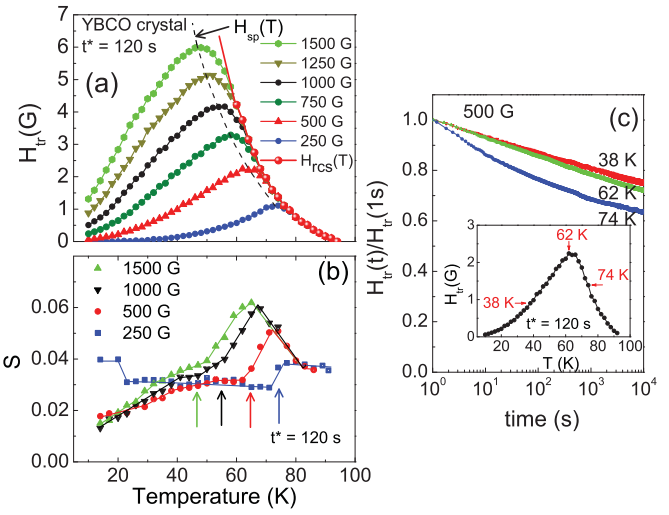

FIG. 2. (Color online) (a) Temperature dependence of the field trapped at the center of the YBCO single crystal by applying different constant magnetic fields between 250 and 1500 G during a time interval t^* of 120 s. $H_{rcs}(T)$ represents the "remanent critical state" line. $H_{sp}(T)$ line joins the maxima of the trapped field. (b) Temperature dependence of the logarithmic decay rates $S = d(\ln H_{tr})/d(\ln t)$ of the trapped field calculated for a short initial time intervals up to 10–20 s. The arrows indicate temperatures at which the maxima in the trapped field occur. (c) Dependence of the field trapped in the YBCO crystal on time measured at different temperatures around the maximum of the trapped field.

generated by the distribution of trapped persistent currents circulating inside this sample.[5,6] The latter fields are related to the currents through the Biot-Savart equations. In the critical state, the sample is completely filled with loops of the "trapped" persistent current at the J_c level. Below the critical state, however, the fields due to the vortex distributions can be simulated using the superposition of the self-fields generated by the "trapped" persistent currents (which circulate at the critical level near the sample's edges), and the "shielding" persistent currents (which circulate near the sample's center in the direction opposite to that of the "trapped" persistent current). At the sample's center, the trapped self-field due to the currents has an axial component only, i.e., its radial component is zero. Its direction is therefore unaffected by the changes of the curvature of magnetic flux lines with an increasing distance from the surface. A magnetic sensor (an axial-radial Hall sensor) placed above the sample's surface at this location could be used to detect this trapped self-field (H_{tr}), which according to the Biot-Savart equations is proportional to the net bulk-trapped current and a geometric factor that depends on the distance between the sensor and the sample's surface. In our experiments, we used an axial-radial Hall sensor of sensitivity ±2 mG, which was positioned 2.5 mm above the sample outside the cryostat, in the air and at the room temperature. We adopted this sensor to measure H_{tr} above the sample's center where H_{tr} has an axial component (parallel to the c-axis) only.

The temperature dependencies of the trapped field H_{tr} obtained by applying different constant magnetic fields H_a to the sample over a fixed time interval t^* are shown in Figs. 1(a), 2(a), and 3(a) for the BSCCO and the YBCO samples. $H_{tr}(T)$ exhibits a maximum at temperatures below the $H_{rcs}(T)$ line which represents the "remanent critical state", i.e., the temperature dependence of the maximum field that could be trapped at the sample's center at each temperature.

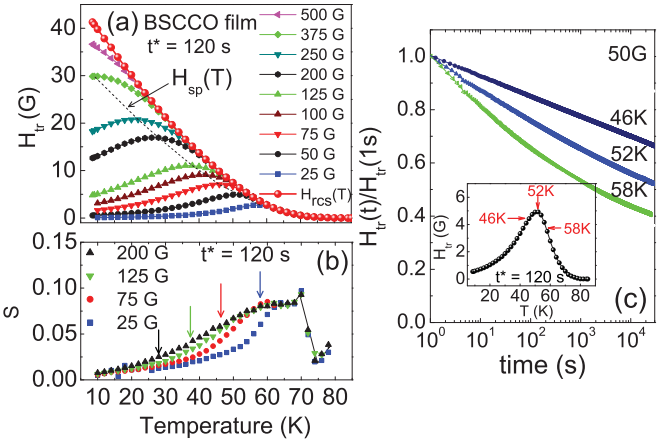

FIG. 3. (Color online) (a) Temperature dependence of the field trapped at the center of the BSCCO thin film by applying magnetic fields between 25 and 500 G during a time interval t^* of 120 s. $H_{rcs}(T)$ represents the "remanent critical state" line. $H_{sp}(T)$ line joins the maxima of the trapped field. (b) Temperature dependence of the logarithmic decay rates $S = d(\ln H_{tr})/d(\ln t)$ of the trapped field calculated for short initial time intervals up to 10–20 s. The arrows indicate temperatures at which the maxima in the trapped field occur. (c) Dependence of the field trapped in the BSCCO film on time measured at different temperatures around the maximum of the trapped field.

The $H_{sp}(T)$ line (dashed curve) joins the maxima of the trapped field. The $H_{sp}(T)$ line approaches the remanent critical state line at high temperatures.

Measurements of the time dependence of the trapped field H_{tr} have been performed for all samples over a time period of up to about $\sim 10^4$ s. They revealed that the decays are logarithmic only at temperatures below the peak in the temperature dependence of the trapped field [see Figs. 1(c), 2(c), and 3(c)]. As discussed below, whether the decay is logarithmic or not provides information on the nature of the vortex interactions. For temperatures at and above the peak, the decay curves start to deviate from the logarithmic behavior observed below the peak. The decay curves at $H_{rcs}(T)$ are also nonlogarithmic.

Because of the nonlogarithmic character of these decay curves, we calculated the decay rates $S = d(\ln H_{tr})/d(\ln t)$ only for very short initial time intervals up to 10–20 s. The dependence of S on temperature for the BSCCO crystal (S for disk and ring-shaped single crystals are similar), the YBCO crystal and the BSCCO thin film are shown in Figs. 1(b), 2(b), and 3(b). The temperature dependence of S calculated for the BSCCO single crystal differs from that obtained for the BSCCO thin film.

Below, we discuss the temperature dependence of the trapped field H_{tr} and that of the decay rates S measured in the pure BSCCO and YBCO single crystals, and analyze the similarities and differences observed. This discussion is followed by the analysis of the relaxation rates in the BSCCO film.

In general, when the applied field H_a is kept constant, one could expect the trapped vortex field to increase with an increasing temperature. Since H_{c1} decreases with an increasing temperature, the surface screening effect becomes weak,[7] allowing more vortices to enter the bulk of the superconductor.[8] The shear modulus of the vortex lattice $c_{66} \approx (\Phi_0 B)/(\pi\lambda)$, where Φ_0 is the flux quantum and B is the magnetic field,[9] also decreases with an increasing temperature due to the increase in the penetration depth λ. Consequently, the vortex lines become flexible which allows some parts of the individual flux lines to deviate from an ideal periodic arrangement of the Abrikosov lattice. The vortex lines then lower their energy by passing through favorable random bulk pinning sites, resulting in an effective trapping.

In addition to the bulk pinning, surface pinning[10–12] and geometrical barriers[13–16] could contribute to the observed pinning of the trapped field. It has been suggested that the surface[1] and geometrical barriers could play a role in determining the vortex dynamics in superconducting single crystals.[17] It has been shown that these barriers lead to an increase of an internal trapped field of crystals at temperatures close to T_c, where the bulk pinning is weak.[13]

The maximum in the dependence of H_{tr} on temperature shown in Figs. 1(a), 2(a), and 3(a) is the result of the competition between vortex entry and bulk pinning. Higher temperatures facilitate vortex entry; however, they also reduce bulk pinning. The vortex lines that enter the superconductor at low temperatures are initially trapped near the edges of the sample. When the temperature is increased, the incoming flux fronts propagate toward the center of the sample, where H_{tr} increases. Eventually above a certain temperature T_{sp}, the sample is fully penetrated by the vortex lines when the flux fronts reach the sample's center. Above this temperature, bulk pinning dominates and consequently H_{tr} drops with an increasing temperature, forming a maximum in $H_{tr}(T)$ at T_{sp} [see the H_{sp} line in Figs. 1(a), 2(a), and 3(a)].

Changes in the vortex pinning as a function of temperature can be seen in the dependence of S on temperature shown for the pure BSCCO and YBCO crystals in Figs. 1(b) and 2(b). $S(T)$ of those samples is characterized by three different regimes.

At temperatures below T_{sp}, marked by arrows in Figs. 1(b) and 2(b) for different applied fields, the samples are in the partial vortex penetration regime. Vortex pinning centers allow for the formation of vortex density gradients, which are equivalent to a current density J. The highest vortex density gradients correspond to the situation where the pinning force acting on a vortex matches the driving Lorentz force, and J reaches the critical value J_c. The vortex density gradients decay due to thermal activation of the vortices over the pinning barrier. In the partial vortex penetration regime, the gradients of the magnetic flux trapped at the sample's edges lead to the outward (out of the sample) and inward (toward the sample's center) motions of the vortex lines.

Consequently, S measured at the sample's center is reduced and its temperature dependence should be weak. This type of behavior has been seen in both the YBCO and the BSCCO crystals after a field of 250 G was applied. S in these crystals is almost independent of temperature at temperatures below T_{sp}. It has been shown that for samples in the remanent state, the "outward" gradients of the flux trapped near the sample's edges are close to the critical values.[6] The "inward" gradients increase when higher magnetic fields are applied, causing a drop of the relaxation rates to even smaller values. This has been observed for both the YBCO and the BSCCO crystals after applying fields higher than 250 G [see Figs. 1(b) and 2(b)]. In this regime, an increase of S with an increasing temperature over a temperature range of 10–15 K for these two cases is about 0.02 for the BSCCO crystal, but only about 0.010 for the YBCO crystal. This reflects the weaker dependence of the pinning potential on temperature and magnetic field in the YBCO crystal compared to that in the BSCCO crystal.

Since the density of the trapped vortex lines is low for all fields that have been applied, the vortices can be trapped by the random pinning centers and there is little interaction between them. The decay of this trapped field is logarithmic, which is in agreement with classical theories of the vortex motion in the absence of vortex-vortex interaction.[18,19]

At temperatures above T_{sp}, the sample is fully penetrated by the vortex lines, and the trapped flux decreases with an increasing temperature. This behavior is dominated by the temperature dependence of the bulk vortex pinning. For example, in the BSCCO crystal, the pinning drops sharply and S rises sharply with an increasing temperature. We believe that this behavior determines the width of a maximum in the temperature dependence of H_{tr} [see Figs. 1(a) and 2(a)]. This width depends on the pinning strength, and consequently is much broader in the YBCO crystal (strong pinning) than in the BSCCO crystal (weak pinning). The decay rates in this regime are nonlogarithmic, which indicates strong vortex-vortex interactions. This type of magnetic relaxation is in

agreement with collective flux creep theories[20–22] and vortex glass theories.[23–25]

At still higher temperatures above T_{sp} closer to T_c, a maximum at a temperature T_{sb} in the temperature dependence of S is observed. At temperatures above T_{sb}, S decreases due to possible effect of surface/geometrical barriers, which dominate at higher temperatures where the bulk pinning is weak.[4]

The magnitudes of the trapped field H_{tr}, and that of H_{rcs} in BSCCO thin film are considerably higher than those found in the pure BSCCO or YBCO crystals. This is related to the sample purity, i.e., thin films contain more defects than crystals. Point defects in the thin film and/or in the interface between the thin film and the substrate could act as stronger pinning centers. Artificial defects introduced into BSCCO by proton irradiation[26] also cause an increase in H_{rcs}. The magnitudes of H_{tr} and H_{rcs} are controlled by the number of pinning centers, as well as by the strength of the pinning potential. The decay rates S for the BSCCO film [Fig. 3(b)] are much smaller than those observed for the BSCCO crystal [Fig. 1(b)] implying that the vortex lines in the film are pinned by defects of stronger pinning potential than those in the pure crystal. On the other hand, pinning of the vortex lines in pure YBCO crystal is stronger than in the BSCCO film, as suggested by the smaller relaxation rates in YBCO [Fig. 2(b)]. Vortex pinning in BSCCO is weaker than that in YBCO in view of the layered vortex structure in two-dimensional BSCCO, which is sensitive to thermal fluctuations and consists of weakly coupled two-dimensional pancake vortices.[27]

In summary, we studied vortex penetration and vortex trapping (vortex remanent state) in BSCCO and YBCO single crystals, and in BSCCO thin films, with the emphasis on the effects of temperature and applied magnetic field. A maximum in the trapped vortex field $H_{tr}(T)$, observed at temperatures a few degrees below those corresponding to the remanent critical state $H_{rcs}(T)$ line, separates the partial vortex penetration regime at low temperatures from the complete vortex penetration regime at high temperatures. The resultant trapped vortex fields at temperatures below and above the maximum are characterized by the logarithmic and nonlogarithmic decays, respectively. At temperatures close to T_c surface/geometrical barriers contribute to these relaxations.

We are grateful to J. R. Clem for useful comments. This work was supported by NSERC.

*jjung@ualberta.ca

[1] C. P. Bean, Phys. Rev. Lett. **8**, 250 (1962).
[2] E. Zeldov, D. Majer, M. Konczykowski, V. B. Geshkenbein, V. M. Vinokur, and H. Shtrikman, Nature **375**, 373 (1995).
[3] Rongchao Ma, A. I. Mansour, M. Egilmez, C. E. Winterfield, I. Fan, K. H. Chow, J. Jung, D. Prabhakaran, and F. Razavy, J. Appl. Phys. **107**, 083909 (2010).
[4] M. Niderost, A. Suter, P. Visani, A. C. Mota, and G. Blatter, Phys. Rev. B **53**, 9286 (1996).
[5] H. Darhmaoui and J. Jung, IEEE Trans. Appl. Supercond. **13**, 2897 (2003).
[6] E. Zeldov, J. R. Clem, M. McElfresh, and M. Darwin, Phys. Rev. B **49**, 9802 (1994).
[7] W. Meissner and R. Ochsenfeld, Naturwissenschaften **21**, 787 (1933).
[8] Ch. Jooss, J. Albrecht, H. Kuhn, S. Leonhardt, and H. Kronmuller, Rep. Prog. Phys. **65**, 651 (2002).
[9] M. Tinkham, *Introduction to Superconductivity* (McGraw-Hill, New York, 1996).
[10] L. Burlachkov, Phys. Rev. B **47**, 8056 (1993).
[11] S. T. Weir, W. J. Nellis, Y. Dalichaouch, B. W. Lee, M. B. Maple, J. Z. Liu, and R. N. Shelton, Phys. Rev. B **43**, 3034 (1991).
[12] N. Chikumoto, M. Konczykowski, N. Motohira, and A. P. Malozemoff, Phys. Rev. Lett. **69**, 1260 (1992).
[13] E. Zeldov, A. I. Larkin, V. B. Geshkenbein, M. Konczykowski, D. Majer, B. Khaykovich, V. M. Vinokur, and H. Shtrikman, Phys. Rev. Lett. **73**, 1428 (1994).
[14] M. V. Indenbom, G. D'Anna, M. O. Andre, V. V. Kabanov, and W. Benoit, Physica C **235–240**, 201 (1994).
[15] M. Benkraouda and J. R. Clem, Phys. Rev. B **53**, 5716 (1996).
[16] E. H. Brandt in *Physics and Materials Science of Vortex State, Flux Pinning and Dynamics*, edited by R. Kossowsky, S. Bose, V. Pan, and Z. Durusoy, NATO Science Series E: Applied Sciences, Vol. 356, pp. 81–108 (Kluwer Academic Publisher, the Netherlands, 1999).
[17] H. Beidenkopf, N. Avraham, Y. Myasoedov, H. Shtrikman, E. Zeldov, B. Rosenstein, E. H. Brandt, and T. Tamegai, Phys. Rev. Lett. **95**, 257004 (2005).
[18] P. W. Anderson, Phys. Rev. Lett. **9**, 309 (1962).
[19] K. Fossheim and A. Sudbo, in *Superconductivity Physics and Applications* (Wiley, England, 2004), p. 206.
[20] Y. Yeshurun and A. P. Malozemoff, Phys. Rev. Lett. **60**, 2202 (1988).
[21] M. V. Feigel'man, V. B. Geshkenbein, and V. M. Vinokur, Phys. Rev. B **43**, 6263 (1991).
[22] M. V. Feigel'man, V. B. Geshkenbein, A. I. Larkin, and V. M. Vinokur, Phys. Rev. Lett. **63**, 2303 (1989).
[23] M. P. A. Fisher, Phys. Rev. Lett. **62**, 1415 (1989).
[24] A. P. Malozemoff and M. P. A. Fisher, Phys. Rev. B **42**, 6784 (1990).
[25] D. S. Fisher, M. P. A. Fisher, and D. A. Huse, Phys. Rev. B **43**, 130 (1991).
[26] L. Krusin-Elbaum, J. R.Thompson, R. Wheeler, A. D. Marwick, C. Li, S. Patel, D. T. Shaw, P. Lisowski, and J. Ullman, Appl. Phys. Lett. **64**, 3331 (1994).
[27] G. Blatter, M. V. Feigelman, V. B. Geshkenbein, A. I. Larkin, and V. M. Vinokur, Rev. Mod. Phys. **66**, 1125 (1994).